Published in final edited form as:
Cancer Lett. 2007 August 18; 253(2): 273–281. doi:10.1016/j.canlet.2007.02.007.

Bombesin Induces Angiogenesis and Neuroblastoma Growth

Jung-Hee Kang, B.S.[1], **Titilope A. Ishola, B.S.**[1], **Naira Baregamian, M.D.**[1], **Joshua M. Mourot, B.S.**[1], **Piotr G. Rychahou, M.D.**[1], **B. Mark Evers, M.D.**[1,2], and **Dai H. Chung, M.D.**[1,2]

[1]Department of Surgery, The University of Texas Medical Branch, 301 University Boulevard, Galveston, Texas 77555, USA

[2]Sealy Center for Cancer Cell Biology, The University of Texas Medical Branch, 301 University Boulevard, Galveston, Texas 77555, USA

Abstract

Gastrin-releasing peptide (GRP), the mammalian equivalent of bombesin (BBS), is a trophic factor for highly vascular neuroblastomas; its mechanisms of action *in vivo* are unknown. We sought to determine the effects of BBS on the growth of neuroblastoma xenografts and on angiogenesis. BBS significantly increased the growth of SK-N-SH and BE(2)-C human neuroblastomas; tumors demonstrated increased expression of angiogenic markers, PECAM-1 and VEGF, as well as phosphorylated (p)-Akt levels. RC-3095, a BBS/GRP antagonist, attenuated BBS-stimulated tumor growth and angiogenesis *in vivo*. GRP or GRPR silencing significantly inhibited VEGF as well as p-Akt and p-mTOR expression *in vitro*. Our findings demonstrate that BBS stimulates neuroblastoma growth and the expression of angiogenic markers. Importantly, these findings suggest that novel therapeutic agents, targeting BBS-mediated angiogenesis, may be useful adjuncts in patients with advanced-stage neuroblastomas.

Keywords

Bombesin; GRP; neuroblastoma; angiogenesis; VEGF

Introduction

Neuroblastoma is the most common extracranial solid tumor in infants and children, accounting for more than 8-10% of all childhood cancers [1]. In particular, patients older than one year of age often present with more aggressive disease and have a dismal prognosis [1,2]. This subset of advanced-stage tumors, and the resultant metastases, are characterized by florid vascularization, which contributes to a rapid tumor progression [3,4]. Vascular endothelial growth factor (VEGF) is a key mediator of carcinogenic neovascularization, and has been associated with poor prognosis in solid tumors [4-8]. VEGF and its receptors are also expressed in human neuroblastoma tumors and cell lines [4,9,10]. Higher levels of VEGF in neuroblastomas correlate with unfavorable histology and aggressive tumor behavior [4,10]. However, the exact cellular mechanisms involved in stimulation of angiogenesis and tumor progression in neuroblastomas are relatively unknown.

Correspondence: Dai H. Chung, M.D., The University of Texas Medical Branch, 301 University Blvd., Galveston, Texas 77555, Tel.: (409) 772 2307, Fax: (409) 772 4253, Email: E-mail: dhchung@utmb.edu.

Derived from neuroendocrine precursor cells, neuroblastomas produce and respond to various hormones, including gastrin-releasing peptide (GRP) [11]. We have previously shown that GRP stimulates neuroblastoma cell growth by an autocrine and/or paracrine mechanism [12]. We also found that the expression of GRP receptor (GRPR), a member of the G-protein coupled receptor (GPCR) family, is notably increased in poorly-differentiated neuroblastomas [12]. Bombesin (BBS), the amphibian analogue of GRP, also binds to GRPR with high affinity to stimulate growth [13-16]. However, the intracellular signaling mechanisms involved in these peptide-mediated proliferative processes are unclear.

In this study, we sought to determine the trophic effects of BBS on the growth of neuroblastoma xenografts and to further elucidate BBS-mediated mechanisms of angiogenesis. We determined that exogenous BBS treatment enhances neuroblastoma growth and stimulates mediators of the angiogenic pathway, whereas, inhibition of BBS/GRP with an antagonist, RC-3095, suppresses tumor progression and vascularization. Moreover, small interfering RNA against GRP (siGRP) or GRPR (siGRPR) decreased VEGF expression and secretion in neuroblastoma cells.

Materials and Methods

Reagents

BBS peptide was obtained from Bachem (Torrance, CA). Antibody against VEGF, GRP, platelet endothelial cell adhesion molecule (PECAM)-1, and horseradish peroxidase (HRP)-conjugated secondary antibodies were purchased from Santa Cruz Biotechnology, Inc. (Santa Cruz, CA). Phosphorylated (p)-Akt (Ser473), total Akt, and p-mTOR antibodies were obtained from Cell Signaling Technology (Beverly, MA). GRPR antibody was from Abcam, Inc. (Cambridge, MA). RC-3095, fetal bovine serum (FBS), and β-actin antibody were purchased from Sigma-Aldrich (St. Louis, MO). pEGFP (GFP) vector was obtained from Clontech Laboratories (Mountain View, CA). Non-targeting control siRNA (siNTC), siGRP and siGRPR were purchased from Dharmacon, Inc. (Lafayette, CO). All cell culture related products were from Cellgro Mediatech, Inc. (Herndon, VA), unless otherwise specified. RNAqueous kit was obtained from Ambion, Inc. (Austin, TX). Lipofectamine 2000 and Hanks Balanced Salt Solution (HBSS) were from Invitrogen (Rockville, MD). Cell Counting Kit-8 (CCK-8) was obtained from Dojindo Molecular Technologies, Inc. (Gaithersburg, MD). Reagents for immunohistochemistry were purchased from either Dako Corporation (Carpinteria, CA) or Richard-Allan Scientific (Kalamazoo, MI). Immunoblot polyvinylidene difluoride (PVDF) membrane was from Bio-Rad Laboratories (Hercules, CA). VEGF enzyme-linked immunosorbant assay (ELISA) kit was purchased from R&D Systems, Inc. (Minneapolis, MN).

Cell culture, siRNA, plasmid transfection

Human neuroblastoma cell lines, SK-N-SH and BE(2)-C, were purchased from American Type Culture Collection (Manassas, VA). Cells were maintained in RPMI 1640 or EMEM medium with L-glutamine supplemented with 10% FBS. The cells were maintained at 37°C in a humidified atmosphere of 95% air and 5% CO_2. For siRNA transfection assays, 6×10^6 cells/400 μl for BE(2)-C or 9×10^6 cells/400 μl for SK-N-SH cells were transfected with siNTC, siGRP or siGRPR by electroporation and seeded onto 100 mm dishes. Setup conditions were 400 V, 500 μF for BE(2)-C and 250 V, 950 μF for SK-N-SH cells. The following day, medium was replaced and the cells were replated onto 60 mm dishes ($5\text{-}10 \times 10^5$ cells). Cells were harvested 2 and 3 days after transfection for various assays. For BBS treatment, the cells were seeded onto 6-well plates for 24 h and then maintained in serum-free conditions overnight. After BBS treatment, cells were harvested for immunoblotting. For GFP plasmid transfection, SK-N-SH cells were transfected with Lipofectamine 2000 according to the manufacturer's

instructions. A stable cell line (GFP-SK-N-SH) was established with G418 treatment at a dose of 300 μg/ml for 2 weeks. The transfected clones were identified by FACS A219 cell sorter (BD Biosciences, San Jose, CA) on the basis of GFP fluorescence. GFP expression was ~70%, as determined by fluorescence-activated cell sorting. GFP-SK-N-SH cells were then used for orthotopic xenografts.

RNA isolation and real time RT-PCR

Total cellular RNA extraction was carried out using RNAqueous kit and real-time RT-PCR was performed by the method previously described [17]. Applied Biosystems (Foster City, CA) assays-on-demand 20× assay mix of primers and TaqMan MGB probes (FAM™ dye-labeled) for the target genes, human GRP (NM_002091, Hs00181852_m1), human VEGF (NM_003376, Hs00173626_m1), and pre-developed 18S rRNA (VIC™-dye labeled probe) TaqMan® assay reagent (P/N 4319413E) were utilized.

Xenograft studies

Male athymic nude mice (4-6 weeks old) were obtained from Harlan Sprague Dawley (Indianapolis, IN) and housed in sterile cages in a temperature-controlled pathogen-free room with an alternating 12 h light and dark cycle. The mice were fed autoclaved chow and tap water *ad libitum* and allowed to acclimate for 1 week. All studies were approved by the Institutional Animal Care and Use Committee at UTMB.

In the first experiment, mice were anesthetized using halothane and xenografts were established by subcutaneous (s.c.) injection of 2×10^6 SK-N-SH cells/100 μl HBSS onto the bilateral flanks using a 26-gauge needle. After two days, the mice were randomized into three experimental groups: I (vehicle control; 0.01 M acetic acid in saline) injection only], II (BBS; 10 μg/kg/injection), and III (BBS; 20 μg/kg/injection). All injections were administered intraperitoneal (i.p.) q 8 h. In the second experiment, the mice were anesthetized using halothane and a small left flank incision was created under sterile conditions to expose the kidney. An inoculum of 2×10^6 SK-N-SH cells in 0.1 ml of HBSS was injected into the superior pole of the left kidney using a 27-gauge needle and then the abdominal wound was closed in one layer with staples. After ten days, the mice were randomized into two experimental groups: I (control) and II (BBS; 20 μg/kg/i.p. injection, q 8 h). In the third experiment, xenografts were initiated by s.c. injection of 5×10^5 BE(2)-C cells in 0.1 ml of HBSS onto bilateral flanks of mice using a 26-gauge needle. Two days after injection, the mice were randomized into four groups: I (control), II (BBS; 20 μg/kg/s.c. injection, t.i.d.), III (BBS/GRP antagonist, RC-3095; 10 μg/kg/s.c. injection, q 12 h), and IV (BBS plus RC-3095). For all *in vivo* experiments, tumor growth was assessed bi-weekly by measuring the two greatest perpendicular tumor dimensions with vernier calipers (Mitutoyo, Tokyo, Japan) and body weights were recorded weekly. The tumor volumes were calculated as follows: tumor volume (mm^3) = [tumor length (mm) × tumor width $(mm)^2$]/2. At sacrifice, tumors were excised, weighed, and snap frozen in liquid nitrogen for storage at -80°C until the assay. Blood was also collected for ELISA.

Immunoblotting

Whole-cell lysates or tissues were prepared as previously described [17,18]. Briefly, total protein (30-50 μg/lane) was resolved on NuPAGE Novex 4-12% Bis-Tris gels and electrophoretically transferred to PVDF membranes. Target proteins were detected by using rabbit, mouse or goat anti-human antibodies (1:200-1000 dilutions) for 3 h at room temperature (RT) or overnight at 4°C. The membranes were washed and incubated with secondary antibodies (1:5000 dilution) conjugated with HRP. Immune complexes were visualized using the enhanced chemiluminescence system. Equal protein loading was confirmed by blotting the same membrane with β-actin antibody.

Cell viability assay

SK-N-SH and BE(2)-C cells were seeded onto 96-well plates (8-12 × 10^3 cells/well) in RPMI 1640 or EMEM culture medium with 10% FBS. The following day, either serum-free medium only or BBS in serum-free medium was added. Cell viability was assessed 3 days after treatment using CCK-8 assay kit. In this tetrazolium-based assay, the formazan dye produced by metabolically active cells was quantified by measuring the absorption of dye solution in a scanning multi-well spectrophotometer at 450 nm. The values, corresponding to the number of viable cells, were read at OD 450 nm. Experiment was repeated three times, and similar results were obtained.

Immunohistochemistry

Neuroblastoma xenografts were fixed in formalin overnight and embedded in paraffin wax. Tumor sections (5 μm) were mounted on glass slides. Sections were de-paraffinized with xylene, rehydrated with ethanol, antigen retrieval performed with 10 mM sodium citrate buffer, and then blocked with blocking solution, for 20 min at RT. Slides were incubated with primary antibodies (VEGF or PECAM-1) overnight at 4°C. They were washed with buffer three times for 5 min each and incubated with secondary antibodies for 30 min at RT. Sections were developed with DAB reagent. The reaction was terminated by immersing slides in dH_2O and sections were counterstained in hematoxylin. Slides were then dehydrated with ethanol and xylene. Coverslips were mounted and slides were left to dry.

VEGF ELISA

For *in vitro* studies, supernatant of cultured cells was collected 3 days after transfection. For *in vivo* studies, mice blood was collected into tubes with EDTA to prevent coagulation, centrifuged at 2 × 10^3 rpm at RT for 15 min, and plasma was stored at -80°C. For assay, plasma samples were thawed, centrifuged, and VEGF levels were measured using human VEGF ELISA kit according to manufacturer's instructions.

Statistical analyses

Tumor size and body weight were analyzed using analysis of variance (ANOVA) for a two-factor experiment with repeated measures on time in SK-N-SH *in vivo* experiments. All effects were assessed at the 0.05 level of significance and all interactions of the effects were assessed at the 0.15 level of significance as the experiment-wise error rates. Fisher's least significant difference procedure was used for multiple comparisons with 0.005 as the comparison-wise error rate. Data analysis was conducted using PROC MIXED with LSMEANS option and Satterthwaite approximation for the denominator degrees of freedom in SAS®, Release 9.1 (SAS Institute Inc., Cary, NC). In BE(2)-C *in vivo* experiments, the *p* values were analyzed by one-way ANOVA for comparison among the treatment groups. Image J (NIH) was used to perform the densitometric analysis of protein expression from immunoblots. A *p* value of < 0.05 was considered significant.

Results

Bombesin increases SK-N-SH cell growth and VEGF expression

BBS is a trophic factor for a host of cancers, including breast, colon, and prostate [16]; its role in angiogenesis in neuroblastoma is not well understood. We sought to determine the trophic and angiogenic effects of BBS on human neuroblastoma cells. BBS treatment for 3 days significantly increased cell viability by 15% in SK-N-SH cells (Fig. 1A). As shown in Figure 1B, this increase was associated with a nearly 5 fold upregulation of VEGF expression. We also found that p-Akt, a known upstream regulator of VEGF [19], was rapidly increased by 7 fold at 5 min after BBS treatment (Fig. 1C). Similar to SK-N-SH, another human neuroblastoma

cell line, BE(2)-C, also showed a significant increase in cell viability after BBS treatment (data not shown). These results demonstrate that BBS is an important stimulator of the angiogenic pathway and growth in neuroblastoma cells.

Bombesin stimulates growth of SK-N-SH xenografts

To further assess the growth stimulatory actions of BBS on neuroblastoma, we next examined the effects of BBS on neuroblastoma xenografts. SK-N-SH cells were injected onto bilateral flanks subcutaneously in athymic nude mice and then mice were randomized to receive either vehicle or BBS. Tumor volume was measured twice weekly and the xenografts were observed daily until sacrifice. As shown in Figure 2A, SK-N-SH tumor volume was significantly increased by treatment day 40 in mice receiving BBS injections at a dosage of 20 μg/kg q 8 h when compared to the control group receiving vehicle alone. Mice receiving BBS at a lower dosage of 10 μg/kg/injection also showed appreciably enhanced tumor volume by treatment day 40; this significant growth stimulatory effect of BBS was delayed to day 43 when compared to the higher dosage of BBS. The trophic actions of BBS were sustained until the end of treatment at day 45. Interestingly, BBS stimulation of SK-N-SH tumor growth was similar with either 10 or 20 μg/kg dosage after 43 days of treatment. At sacrifice, tumor weight in mice receiving BBS correlated with tumor volume data; however, a statistical difference in tumor weight was noted only in the higher BBS dosage group (20 μg/kg) due to considerable tumor size variability (Fig. 2B). We next wanted to further examine the trophic actions of BBS in orthotopically-established SK-N-SH tumors. We chose the BBS dosage of 20 μg/kg/injection based on our previous experiment. Similar to the heterotopic xenograft study, significantly increased growth was noted in the orthotopic xenografts of mice treated with BBS at 6 weeks (Figs. 2C, D), further confirming the role of BBS as a trophic factor for neuroblastoma growth *in vivo*.

Bombesin induces the expression of angiogenic markers in SK-N-SH in vivo

In order to elucidate the effects of BBS on angiogenesis *in vivo*, we analyzed SK-N-SH heterotopic tumor sections for VEGF, an important signaling protein involved in both vasculogenesis and angiogenesis, and PECAM-1, a marker for microvessels. As shown in Figure 3A, BBS-treated tumors showed enhanced expression of VEGF. Moreover, BBS-treated tumors also showed increased expression of PECAM-1 (Fig. 3B). For both immunohistochemical studies, VEGF and PECAM-1 appeared as dark brown staining in blood vessels and adjacent tissues. In addition, there was also an enhanced p-Akt expression by nearly 2-fold in SK-N-SH tumors as noted by Western blot analysis at sacrifice following BBS treatment (Fig. 3C). These data confirm our *in vitro* findings and further support our hypothesis that BBS regulates angiogenesis in neuroblastoma.

GRP antagonist inhibits BE(2)-C growth and VEGF expression in vivo

BBS upregulation of angiogenic markers was further confirmed using an antagonist to BBS/GRP *in vivo*. Human neuroblastoma BE(2)-C cells were implanted subcutaneously in athymic nude mice. Mice were then randomized to receive vehicle, BBS, and/or the BBS/GRP antagonist, RC-3095. As shown in Figure 4A, RC-3095 treatment significantly suppressed BE(2)-C neuroblastoma growth when compared to BBS treatment alone or control group. Additionally, RC-3095, in combination with BBS, also attenuated tumor growth comparable to control group (Fig. 4A). Western blot analysis showed induction of VEGF (3.2-fold) and p-Akt (2.2-fold) protein expression in BBS-treated mice when compared to vehicle treated mice (Fig. 4B). Correlative to tumor volume inhibition, RC-3095 treatment also blocked BBS-mediated VEGF and p-Akt expression (Fig. 4B). When tumor sections were examined for VEGF protein expression using immunohistochemistry, RC-3095 treatment significantly attenuated BBS-induced increases in VEGF expression in BE(2)-C xenografts (Fig. 4C),

further suggesting an important role of BBS as an inducer of angiogenesis in neuroblastomas. As shown in Figure 4D, ELISA analysis of plasma VEGF levels also clearly demonstrated significantly suppressed levels of plasma VEGF with RC-3095 treatment, alone and/or in combination with BBS. This further suggests BBS as a pro-angiogenic factor for neuroblastomas *in vivo*. In all three *in vivo* experiments, mice tolerated the injections of either BBS or RC-3095 without any detectable systemic toxicity.

GRP/GRPR silencing inhibits angiogenic effectors in neuroblastoma cells

We next assessed the effects of endogenous GRP or GRPR knockdown on VEGF expression. SK-N-SH and BE(2)-C cells were transfected with either siGRP, siGRPR or siNTC. Efficacy of siGRP transfection in SK-N-SH cells was confirmed by quantitative RT-PCR, which showed significantly decreased GRP mRNA levels (Fig. 5A). Transfection efficacy of siGRP in BE (2)-C cells was confirmed by Western blotting (Fig. 5B). Western blot analysis showed a significant decrease in VEGF protein expression with GRP silencing when compared to siNTC in both SK-N-SH and BE(2)-C cells (Fig. 5A, B). This was also associated with a decrease in upstream regulators of the angiogenic pathway, p-Akt and p-mTOR [19] (Fig. 5A, B). As shown in Figure 5C, VEGF mRNA levels were significantly decreased in BE(2)-C cells transfected with siGRP, suggesting regulation of VEGF at the transcription level. This decrease in mRNA levels correlated with marked reduction in VEGF secretion into cell culture media with GRP knockdown (Fig. 5C). Since GRP binds with high affinity to its receptor GRPR, we then transfected BE(2)-C cells with siGRPR to confirm GRP/GRPR-mediated angiogenic effects in neuroblastoma cells. Transfection efficacy of siGRPR in BE(2)-C cells was confirmed by Western blotting. We also noted a significant decrease in VEGF protein expression with GRPR silencing when compared to siNTC-transfected cells (Fig. 5D). Consistent with the effects of GRP silencing on VEGF mRNA and secretion, GRPR knockdown in BE(2)-C cells also showed a reduction of VEGF mRNA as well as its peptide secretion into the cell culture media (Fig. 5D), further confirming that specific GRP binding to its cell surface receptor, GRPR, is critical to induce VEGF activation in neuroblastoma cells. In addition, similar to our *in vivo* findings with RC-3095, GRP-silenced neuroblastoma cells showed a significant decrease in cell viability in comparison to control cells (data not shown). These results further suggest an angiogenic role for GRP in neuroblastoma progression.

Discussion

In our current study, we show that BBS treatment enhances tumor growth and stimulates the expression of angiogenic markers in neuroblastoma, both *in vivo* and *in vitro*. Inhibition of BBS/GRP with an antagonist, RC-3095, or siRNA significantly suppresses tumor progression and vascularization. Moreover, BBS induces activation of Akt, a major effector of phosphatidylinositol 3-kinase (PI3K), suggesting an important role for this signaling pathway in the regulation of angiogenesis and growth in neuroblastoma.

Neuroblastomas are archetypical solid tumors, where vascular proliferation is a hallmark and corresponds to tumor prognosis [3,4]. The significance of neovascularization in neuroblastomas is supported by numerous studies on anti-angiogenic strategies [21-24]. In particular, specific blockade of VEGF resulted in the inhibition of tumor growth and decreased recruitment of preexisting blood vessels in neuroblastoma *in vivo* models [22-24]. We have shown that BBS increases angiogenic markers, VEGF and PECAM-1, in neuroblastomas *in vivo* and/or *in vitro*.

Since human neuroblastomas actively secrete GRP [11], the mammalian analogue of BBS, these observations further underscore the relevance of the growth factor properties of GRP. Levine et al. [25], noted that GRP treatment in prostate cancer cells stimulated pro-angiogenic factors NF-κB, IL-8, and VEGF. We have also observed an increase in IL-8 gene transcription

in neuroblastoma cells upon treatment with GRP (Qiao et al., preliminary results). Recently, it was reported that GRP can directly stimulate endothelial cell migration and cord formation *in vitro* and tumor angiogenesis *in vivo*; these effects were reversed upon treatment with a GRP antagonist [26]. The pro-angiogenic property of BBS/GRP was also confirmed in studies in which antagonists decreased angiogenesis in breast cancer, renal cell carcinoma, and glioblastoma models [27-29]. Likewise, we noted a reduction in neuroblastoma tumor size and VEGF expression *in vivo* with RC-3095 (Fig. 4). The antagonist, RC-3095, shows potential for treatment of a number of solid malignancies; however a current phase 1 clinical trial provided promising, yet inconclusive results due to pharmacokinetic concerns [30]. In addition to pharmacologic inhibition, we also noted that GRP silencing in neuroblastoma cells significantly reduced VEGF expression and secretion, while also decreasing protein expression of p-Akt and p-mTOR, upstream regulators of VEGF (Fig. 5). Therefore, we propose that targeting BBS/GRP may prove to be useful as adjuvant treatment in highly vascularized neuroblastomas.

We show that BBS activates the PI3K pathway *in vivo* and *in vitro*. Phosphorylation of Akt, a PI3K downstream effector, regulates cellular signals that are critical for cell survival and angiogenesis [31,32]. Tan et al. [19], showed that PI3K activation up-regulated VEGF expression in prostate cancer cells and that activated Akt stimulates mTOR by phosphorylation and promotes VEGF transcription [19]. We also demonstrate the activation of Akt and mTOR in our model, with subsequent VEGF upregulation. In conclusion, we have, for the first time, demonstrated that BBS stimulates neuroblastoma growth and the expression of angiogenic markers *in vivo*, and have also elucidated possible molecular mechanisms through regulation of PI3K and VEGF signaling pathways. Novel strategies targeting GRP-mediated tumor growth may be beneficial in patients with highly vascularized, advanced-stage neuroblastomas.

Acknowledgments

The authors thank Karen Martin for manuscript preparation and Tatsuo Uchida for statistical analysis. This work was supported by grants RO1 DK61470, RO1 DK48498, RO1 CA104748 and PO1 DK35608 from the National Institutes of Health and an Institutional Research Grant (IRG-110376) from the American Cancer Society.

References

1. Brodeur GM. Neuroblastoma: biological insights into a clinical enigma. Nat Rev Cancer 2003;3:203–216. [PubMed: 12612655]
2. Maris JM, Matthay KK. Molecular biology of neuroblastoma. J Clin Oncol 1999;17:2264–2279. [PubMed: 10561284]
3. Meitar D, Crawford SE, Rademaker AW, Cohn SL. Tumor angiogenesis correlates with metastatic disease, N-myc amplification, and poor outcome in human neuroblastoma. J Clin Oncol 1996;14:405–414. [PubMed: 8636750]
4. Fukuzawa M, Sugiura H, Koshinaga T, Ikeda T, Hagiwara N, Sawada T. Expression of vascular endothelial growth factor and its receptor Flk-1 in human neuroblastoma using in situ hybridization. J Pediatr Surg 2002;37:1747–1750. [PubMed: 12483647]
5. Ferrara N, Gerber HP, LeCouter J. The biology of VEGF and its receptors. Nat Med 2003;9:669–676. [PubMed: 12778165]
6. Foekens JA, Peters HA, Grebenchtchikov N, Look MP, Meijer-van Gelder ME, Geurts-Moespot A, van der Kwast TH, Sweep CG, Klijn JG. High tumor levels of vascular endothelial growth factor predict poor response to systemic therapy in advanced breast cancer. Cancer Res 2001;61:5407–5414. [PubMed: 11454684]
7. Herbst RS, Onn A, Sandler A. Angiogenesis and lung cancer: prognostic and therapeutic implications. J Clin Oncol 2005;23:3243–3256. [PubMed: 15886312]

8. Ishigami SI, Arii S, Furutani M, Niwano M, Harada T, Mizumoto M, Mori A, Onodera H, Imamura M. Predictive value of vascular endothelial growth factor (VEGF) in metastasis and prognosis of human colorectal cancer. Br J Cancer 1998;78:1379–1384. [PubMed: 9823983]
9. Beierle EA, Dai W, Langham MR Jr, Copeland EM 3rd, Chen MK. VEGF receptors are differentially expressed by neuroblastoma cells in culture. J Pediatr Surg 2003;38:514–521. [PubMed: 12632379]
10. Langer I, Vertongen P, Perret J, Fontaine J, Atassi G, Robberecht P. Expression of vascular endothelial growth factor (VEGF) and VEGF receptors in human neuroblastomas. Med Pediatr Oncol 2000;34:386–393. [PubMed: 10842244]
11. Gustafson WC, De Berry BB, Evers BM, Chung DH. Role of gastrointestinal hormones in neuroblastoma. World J Surg 2005;29:281–286. [PubMed: 15706438]
12. Kim S, Hu W, Kelly DR, Hellmich MR, Evers BM, Chung DH. Gastrin-releasing peptide is a growth factor for human neuroblastomas. Ann Surg 2002;235:621–629. [PubMed: 11981207]discussion 629-630
13. Kroog GS, Jensen RT, Battey JF. Mammalian bombesin receptors. Med Res Rev 1995;15:389–417. [PubMed: 8531502]
14. Hellmich MR, Ives KL, Udupi V, Soloff MS, Greeley GH Jr, Christensen BN, Townsend CM Jr. Multiple protein kinase pathways are involved in gastrin-releasing peptide receptor-regulated secretion. J Biol Chem 1999;274:23901–23909. [PubMed: 10446156]
15. Xiao D, Chinnappan D, Pestell R, Albanese C, Weber HC. Bombesin regulates cyclin D1 expression through the early growth response protein Egr-1 in prostate cancer cells. Cancer Res 2005;65:9934–9942. [PubMed: 16267018]
16. Patel O, Shulkes A, Baldwin GS. Gastrin-releasing peptide and cancer. Biochim Biophys Acta 2006;1766:23–41. [PubMed: 16490321]
17. Kang J, Kamal A, Burrows FJ, Evers BM, Chung DH. Inhibition of neuroblastoma xenograft growth by Hsp90 inhibitors. Anticancer Res 2006;26:1903–1908. [PubMed: 16827123]
18. Kang JH, Rychahou PG, Ishola TA, Qiao J, Evers BM, Chung DH. MYCN silencing induces differentiation and apoptosis in human neuroblastoma cells. Biochem Biophys Res Commun 2006;351:192–197. [PubMed: 17055458]
19. Tan C, Cruet-Hennequart S, Troussard A, Fazli L, Costello P, Sutton K, Wheeler J, Gleave M, Sanghera J, Dedhar S. Regulation of tumor angiogenesis by integrin-linked kinase (ILK). Cancer Cell 2004;5:79–90. [PubMed: 14749128]
20. Meister B, Grunebach F, Bautz F, Brugger W, Fink FM, Kanz L, Mohle R. Expression of vascular endothelial growth factor (VEGF) and its receptors in human neuroblastoma. Eur J Cancer 1999;35:445–449. [PubMed: 10448297]
21. Nagabuchi E, VanderKolk WE, Une Y, Ziegler MM. TNP-470 antiangiogenic therapy for advanced murine neuroblastoma. J Pediatr Surg 1997;32:287–293. [PubMed: 9044139]
22. Kim ES, Serur A, Huang J, Manley CA, McCrudden KW, Frischer JS, Soffer SZ, Ring L, New T, Zabski S, Rudge JS, Holash J, Yancopoulos GD, Kandel JJ, Yamashiro DJ. Potent VEGF blockade causes regression of coopted vessels in a model of neuroblastoma. Proc Natl Acad Sci U S A 2002;99:11399–11404. [PubMed: 12177446]
23. Ribatti D, Ponzoni M. Antiangiogenic strategies in neuroblastoma. Cancer Treat Rev 2005;31:27–34. [PubMed: 15707702]
24. Backman U, Christofferson R. The selective class III/V receptor tyrosine kinase inhibitor SU11657 inhibits tumor growth and angiogenesis in experimental neuroblastomas grown in mice. Pediatr Res 2005;57:690–695. [PubMed: 15718357]
25. Levine L, Lucci JA 3rd, Pazdrak B, Cheng JZ, Guo YS, Townsend CM Jr, Hellmich MR. Bombesin stimulates nuclear factor kappa B activation and expression of proangiogenic factors in prostate cancer cells. Cancer Res 2003;63:3495–3502. [PubMed: 12839933]
26. Martinez A, Zudaire E, Julian M, Moody TW, Cuttitta F. Gastrin-releasing peptide (GRP) induces angiogenesis and the specific GRP blocker 77427 inhibits tumor growth in vitro and in vivo. Oncogene 2005;24:4106–4113. [PubMed: 15750618]
27. Bajo AM, Schally AV, Groot K, Szepeshazi K. Bombesin antagonists inhibit proangiogenic factors in human experimental breast cancers. Br J Cancer 2004;90:245–252. [PubMed: 14710236]

28. Heuser M, Schlott T, Schally AV, Kahler E, Schliephake R, Laabs SO, Hemmerlein B. Expression of gastrin releasing Peptide receptor in renal cell carcinomas: a potential function for the regulation of neoangiogenesis and microvascular perfusion. J Urol 2005;173:2154–2159. [PubMed: 15879878]

29. Kanashiro CA, Schally AV, Cai RZ, Halmos G. Antagonists of bombesin/gastrin-releasing peptide decrease the expression of angiogenic and anti-apoptotic factors in human glioblastoma. Anticancer Drugs 2005;16:159–165. [PubMed: 15655413]

30. Schwartsmann G, DiLeone LP, Horowitz M, Schunemann D, Cancella A, Pereira AS, Richter M, Souza F, da Rocha AB, Souza FH, Pohlmann P, De Nucci G. A phase I trial of the bombesin/gastrin-releasing peptide (BN/GRP) antagonist RC3095 in patients with advanced solid malignancies. Invest New Drugs 2006;24:403–412. [PubMed: 16505950]

31. Katso R, Okkenhaug K, Ahmadi K, White S, Timms J, Waterfield MD. Cellular function of phosphoinositide 3-kinases: implications for development, homeostasis, and cancer. Annu Rev Cell Dev Biol 2001;17:615–675. [PubMed: 11687500]

32. Hennessy BT, Smith DL, Ram PT, Lu Y, Mills GB. Exploiting the PI3K/AKT pathway for cancer drug discovery. Nat Rev Drug Discov 2005;4:988–1004. [PubMed: 16341064]

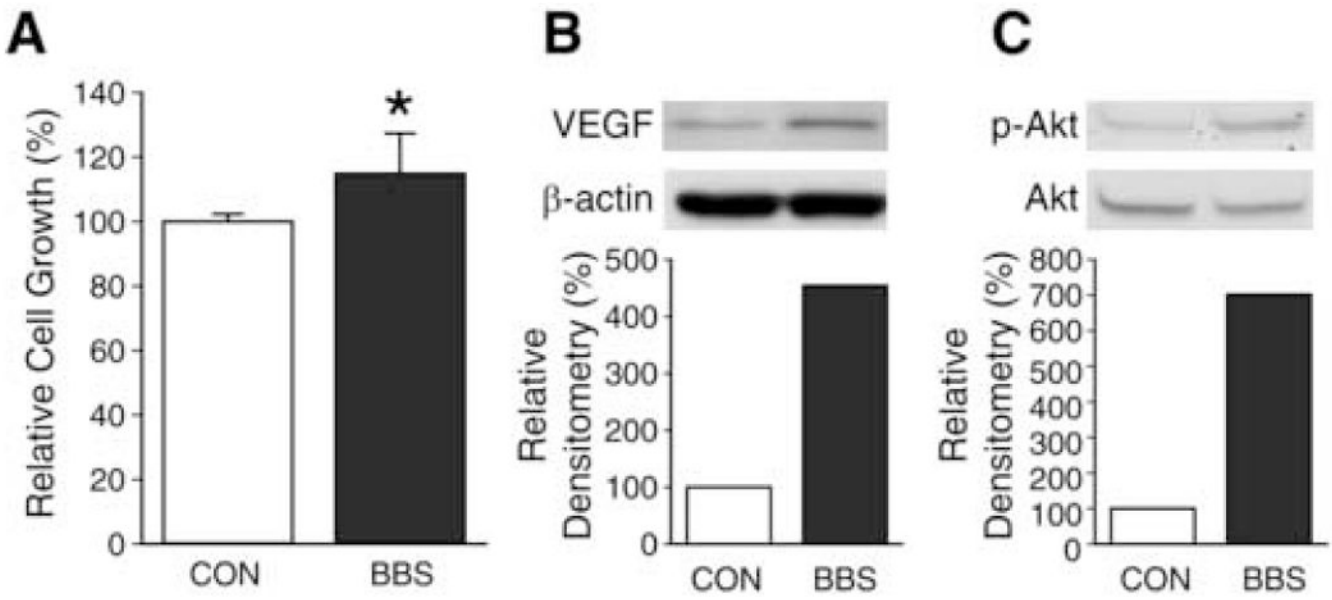

Figure 1. BBS stimulates cell growth, VEGF and p-Akt expression in SK-N-SH cells

(A) Effects of BBS (10^{-7} M) on SK-N-SH cell viability were determined using CCK-8 kit (Data represent mean ± SEM values of eight replicate experiments; * $p < 0.05$ vs. control). (B) SK-N-SH cells were treated with BBS (10^{-7} M) for one day after overnight serum-free conditions. Cell lysates were prepared and analyzed by Western blot for VEGF. (C) SK-N-SH cells were treated with BBS (10^{-7} M) for 5 min after overnight serum-free condition. Cell lysates were prepared and analyzed by Western blot for p-Akt and total Akt. Experiments were repeated on two separate occasions.

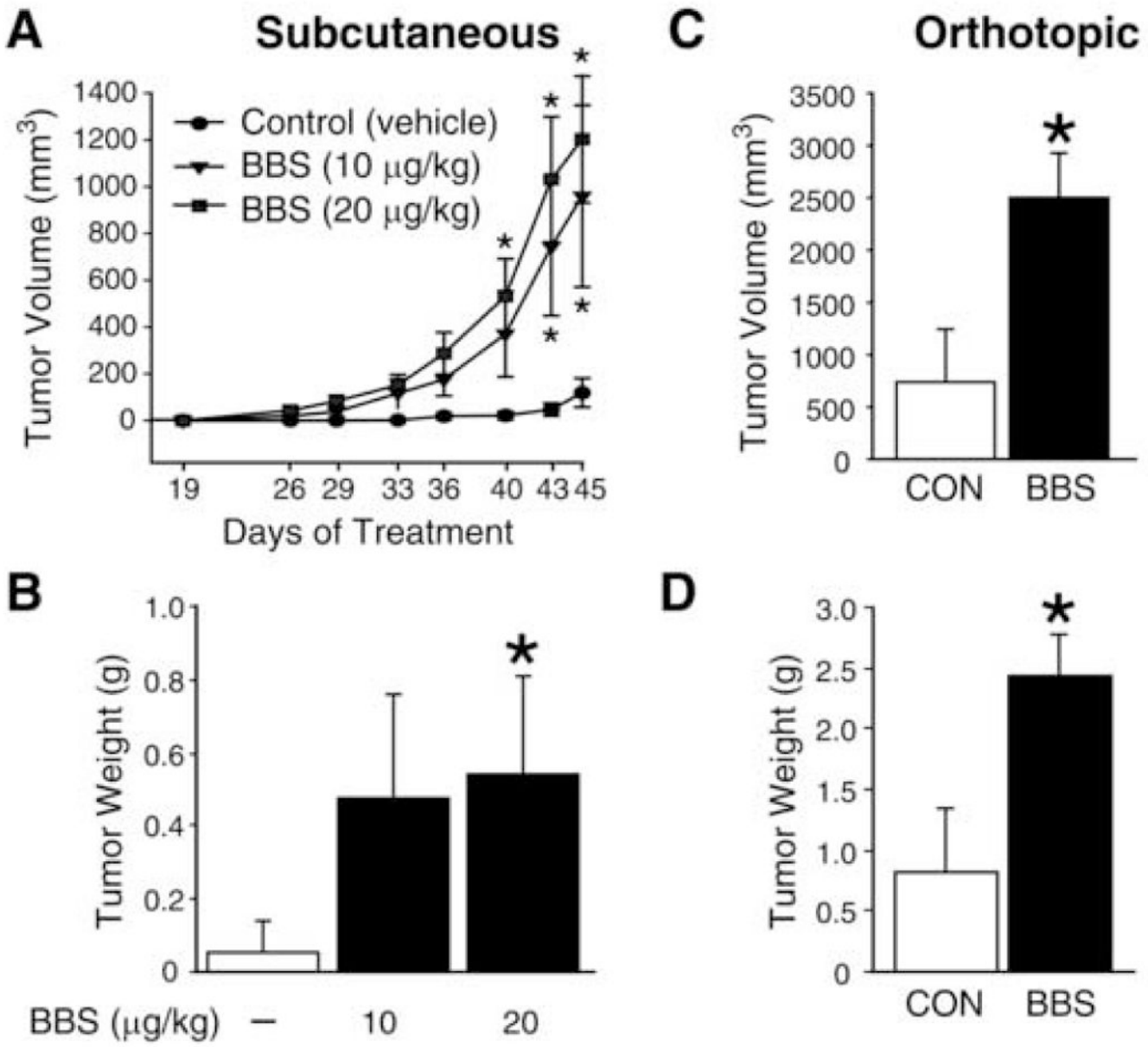

Figure 2. BBS promotes SK-N-SH growth *in vivo*

(A, B) Tumor volumes and tumor weights of subscapular SK-N-SH xenografts in mice treated with vehicle or BBS (i.p.) for 45 days as described in "Materials and Methods" (4-6 mice/group). (C, D) Tumor volumes and tumor weights of orthotopic SK-N-SH xenografts at sacrifice, established by injecting cells into left kidney of mice and treated with vehicle or BBS (20 μg/kg/injection; i.p.) for 43 days as described in "Materials and Methods" (5-6 mice/group). Data from all figures represent mean ± SEM; * $p < 0.05$ vs. control.

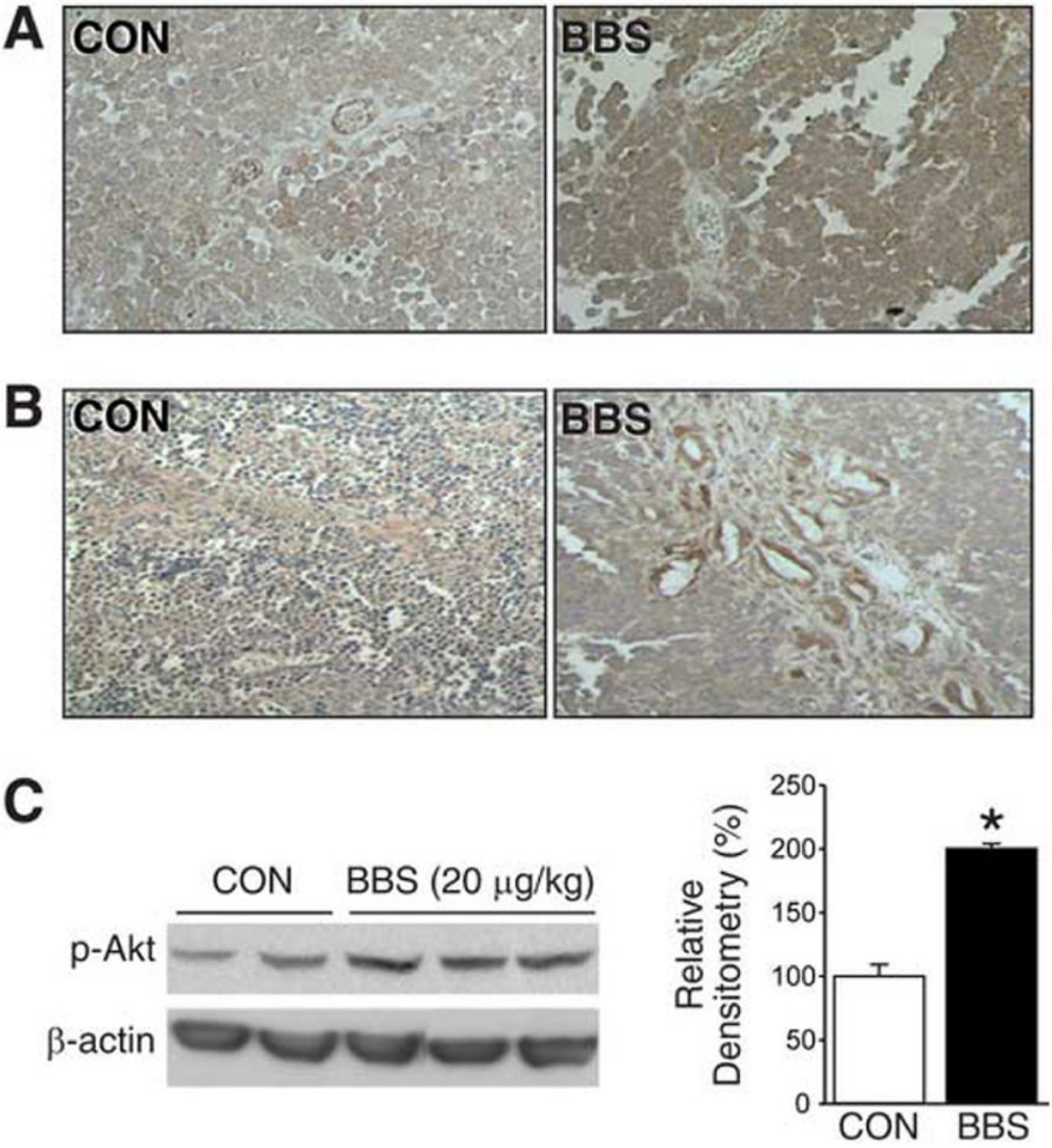

Figure 3. BBS induces angiogenesis in SK-N-SH xenografts

(A) Representative sections of SK-N-SH tumors from vehicle- or BBS-treated mice stained with anti-human VEGF antibody (brown); magnification, X400. (B) Representative sections of SK-N-SH tumors from vehicle- or BBS-treated mice stained with anti-human PECAM-1 antibody (brown); magnification X200. (C) Expression of p-Akt in SK-N-SH tumor tissue samples from mice treated with BBS or vehicle; five representative tumors are shown (Data represent mean ± SEM; * $p < 0.05$ vs. control).

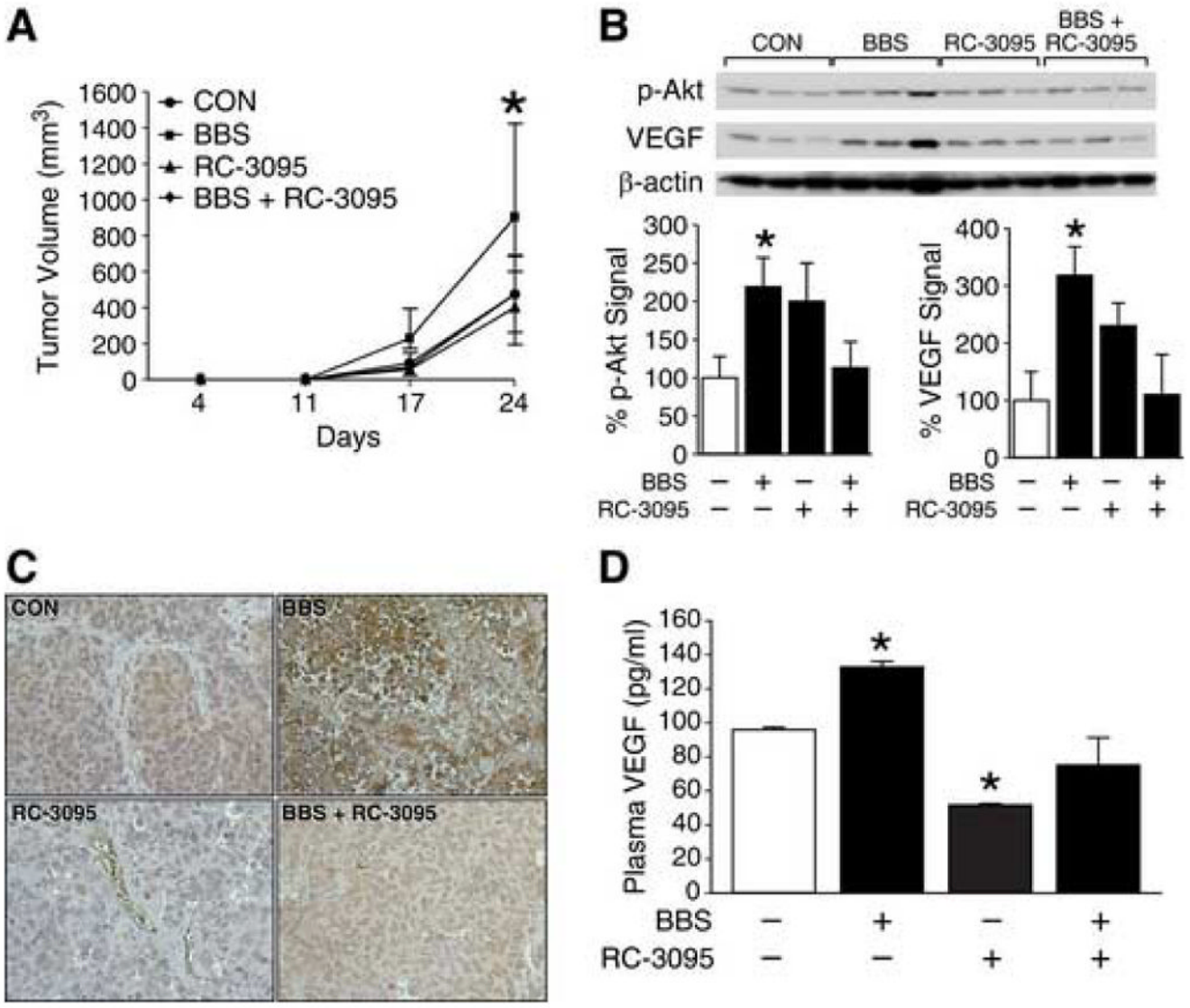

Figure 4. GRP antagonist inhibits BE(2)-C tumor growth and angiogenesis

(A) Tumor volumes in nude mice with BE(2)-C cells treated with vehicle, BBS (20 μg/kg/injection; s.c., t.i.d.), and/or RC-3095 (10 μg/kg/injection; s.c., q 12 h), as described in "Materials and Methods" (5-6 mice/group). (B) Expression of p-Akt and VEGF in BE(2)-C tumor tissue samples (three representative tumor samples from each group are shown). (C) Representative sections of BE(2)-C tumors stained with anti-human VEGF antibody (brown); magnification, X400. (D) VEGF plasma levels from mice detected by ELISA. Data from all figures represent mean ± SEM; * $p < 0.05$ vs. control.

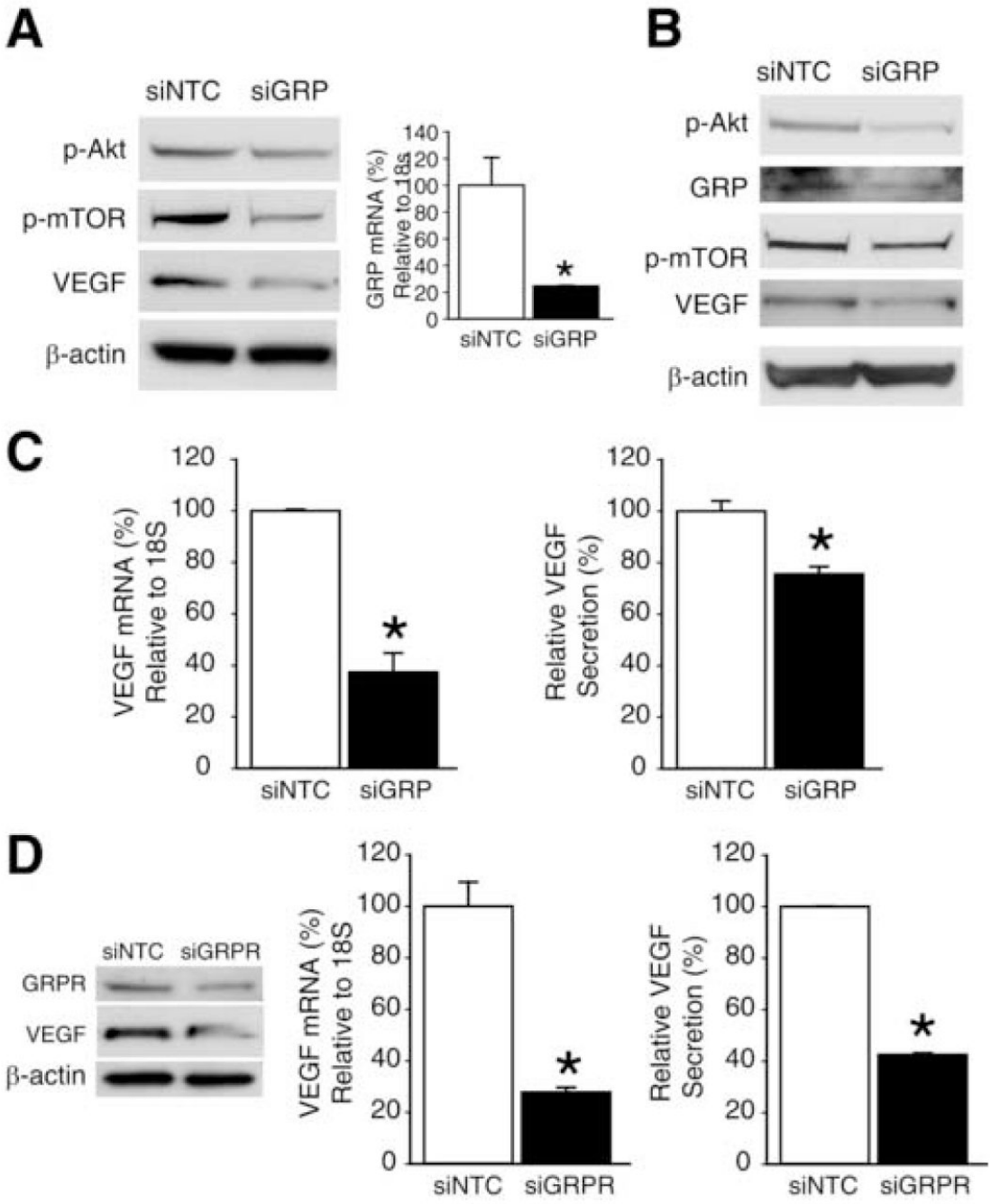

Figure 5. GRP/GRPR siRNA attenuates angiogenesis in human neuroblastoma cells

(A) Western blot analysis of p-Akt, p-mTOR and VEGF protein expression in SK-N-SH cells at 3 d post-transfection with siNTC or siGRP (*left panel*). Quantitative RT-PCR for GRP mRNA levels in SK-N-SH cells at 2 d post-transfection with siNTC or siGRP (*right panel*). (B) Western blot analysis of p-Akt, GRP, p-mTOR and VEGF protein expression in BE(2)-C cells at 3 d post-transfection with siNTC or siGRP. (C) Quantitative RT-PCR analysis for VEGF mRNA level in BE(2)-C cells at 2 d post-transfection with siNTC or siGRP (*left panel*). VEGF levels in BE(2)-C using human VEGF ELISA kit. Cell culture supernatants were harvested at 3 d post-transfection with siNTC or siGRP (*right panel*). (D) BE(2)-C cells were transfected with siNTC or siGRPR for various assays. GRPR and VEGF protein expression

was determined by Western blot analysis at 3 d post-transfection (*left panel*). VEGF mRNA levels were assessed by quantitative RT-PCR at 2 d post-transfection (*middle panel*) and VEGF levels in cell culture supernatants were measured by ELISA at 3 d post-transfection (*right panel*). Data from all figures represent mean ± SEM; * $p < 0.05$ vs. control.